ISSN (Print) 1226-1750
ISSN (Online) 2233-6656
Journal of Magnetics 23(4), 578-583 (2018) https://doi.org/10.4283/JMAG.2018.23.4.578

3D Helmholtz Coil-based Hybrid Manipulation for Active Locomotion of Magnetic Micro/Nano Robots

Sung Hoon Kim*

Department of Electronics Convergence Engineering, Wonkwang University, 460 Iksandae-ro, Iksan, Jeonbuk 54538, Republic of Korea

(Received 21 October 2018, Received in final form 19 December 2018, Accepted 19 December 2018)

This study presents hybrid control based on three-axis Helmholtz coil for manipulation of magnetic micro/nano robots. In general, magnetic force and torque control requires both Maxwell and Helmholtz coils. Therefore, the configuration of the magnetic manipulation system is complex and requires many power supplies. The hybrid method controls the three-axis Helmholtz coil and three power supplies through mechanical switch control to generate magnetic force and torque. Magnetic torque is controlled by the three-axis Helmholtz coil with a rotating magnetic field, and magnetic force is controlled by generating gradient magnetic field through the separated coils by the switch control. Three switches separate each Helmholtz coil and six switches control the separated six coil with the three power supplies. The hybrid control can provide simple configuration of coil system, various active locomotion, and precision control in complex environments. To verify the proposed method, we conducted magnetic simulation with various experimental tests.

Keywords : hybrid control of magnetic force and torque, switch control, Helmholtz coil

1. Introduction

Magnetic micro/nano robots have been developed for minimally invasive treatments because of a wireless manipulation [1-5]. In general, magnetic manipulation is divided into a permanent magnet control (PM control) and an electromagnetic field control (EM control) using coils [6, 7]. The PM control utilizes magnetic force that is depended on distance between the driving magnet and magnetic robot, whereas the EM control has various control parameters: current, distance, frequency, and phase difference. Therefore, the EM control is higher controllability than that of the PM control. The EM control is divided into two types: magnetic force control and magnetic torque control by gradient and uniform magnetic fields, respectively [8, 9]. Magnetic force control generates a translational force by gradient magnetic field, whereas magnetic torque control generates a rotational motion by uniform magnetic field. Therefore, magnetic torque control requires mechanical mechanism to generate active locomotion, such as spiral-type and tail mechanisms [10-14].

In the case of translational motion due to gradient magnetic field, the mobility is not excellent in complex environment because the motion depends only on magnetic force. However, since no mechanical mechanism is required, the size of the robot can be very small. Magnetic torque control requires propulsion mechanisms according to types of magnetic fields. For example, a rotating magnetic field requires a spiral mechanism, and an alternating field requires a tail mechanism to generate propulsive force. Because of mechanical propulsive force, mobility due to magnetic torque control is better than force control [15, 16]. To generate both the translational motion and rotating motion of magnetic robots, the coil system requires a combination of Maxwell coil and Helmholtz coil. In this case, the total configuration of coil system is complex. In addition, the number of the driving power supplies is increased. To avoid these issues, we proposed hybrid control (force and torque control) based on switching control of three-axis Helmholtz coil with three power supplies. The proposed method basically generates a rotating magnetic field using Helmholtz coils for magnetic torque control. When the magnetic force control is performed, the Helmholtz coil is separated through the switch control to generate the gradient magnetic field. For this function, we utilized nine relay switches. Three relay switches can separate three Helmholtz coils (X, Y, and Z axis) into six single coils (X1, X2, Y1, Y2, Z1, and Z2).

*Corresponding author: Tel: +82-63-850-6739
Fax: +82-63-850-6739, e-mail: kshoon@wku.ac.kr

Six relay switches can select the six single coils: X1 or X2, Y1 or Y2, Z1 or Z2 from three power supplies). Through the switch control of Helmholtz coils, we utilized magnetic force and torque to manipulate magnetic microrobot. To verify the performance of hybrid control, we conducted magnetic simulation with various experiments of active locomotion using a spiral-type robot and a cylindrical permanent magnet.

2. Method of Hybrid Control

2.1. Electromagnetic navigation system of hybrid control

For hybrid control of magnetic microrobot, we developed an electromagnetic manipulation system, as shown in Fig. 1. The control system consists of three-axis Helmholtz coil, three power supplies, a control software, a joystick, and switch modules, as shown in Fig. 1(a). Table 1 shows specification of the fabricated three-axis Helmholtz coil. In the coil system, working space for robot control is 60 mm × 60 mm × 60 mm. In general, Helmholtz coil provides magnetic torque control because of generation of a uniform magnetic field. For hybrid control (magnetic torque and force control), the fabricated three-axis Helmholtz coil is connected by relay switches, as shown in Fig. 1 (b). Figure 1(b) shows the switch configuration of X-axis Helmholtz coil. The Y and Z axis coils are equivalent configuration of the X-axis. When the switch S4 is turned ON, the X-axis coil become Helmholtz coil for magnetic torque control, whereas if S4 is turned OFF, the Helmholtz coil is separated into two single coils (X1 and X2). In this case, the two single coils (X1 and X2) are selected by S5 or S6, respectively, to generate a gradient magnetic field. Thus, it is determined by the three switches (S1, S4, and S7) whether it is a Helmholtz coil. The six switches (S2, S3, S5, S6, S8, and S9) select X1_coil or X2_coil, Y1_coil or Y2_coil, and Z1_coil or Z2_coil, respectively. Figure 2(a) shows magnetic simulations of the uniform magnetic fields at X, Y and Z-axis Helmholtz coils according to changes in the applied current signals (2, 6, and 10 A). The coil distances of X1 and X2, Y1 and Y2, and Z1 and Z2 are 87.5 mm, 100 cm, and 75 cm, respectively. The working space is 60 mm from −30 mm to 30 mm. When the applied current is 6 A at X, Y and Z-axis coils, each Helmholtz coil generates the uniform fields of 6.2, 6.3, and 3.8 kA/m, respectively. The coil system (X2, Y2, and Z2 coils) generated a linearly increasing gradient magnetic fields in the working space (−30 to 30 mm), as shown in Fig. 2(b). The X2 coil generates 2.16 kA/m at

Table 1. Specification of helmholtz coils.

Coil	Radius (mm)	Wire diameter (mm)	Number of turn
X axis	87.5	1.2	280
Y axis	100	1.2	320
Z axis	75	1.6	140

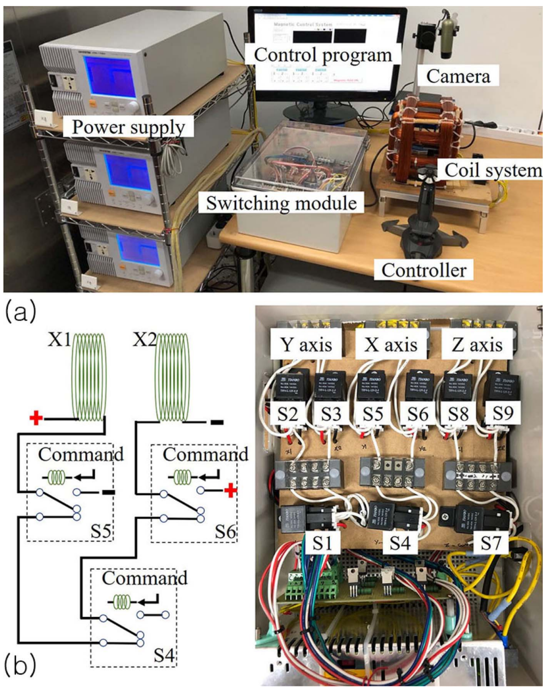

Fig. 1. (Color online) (a) Total hybrid control system and (b) configuration of switch module for hybrid control.

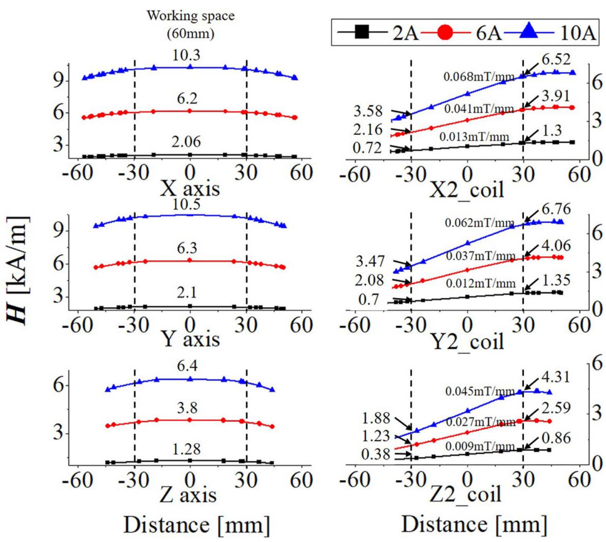

Fig. 2. (Color online) Magnetic simulations for magnetic torque control and force control: (a) uniform magnetic field distribution of three Helmholtz coils, (b) gradient magnetic field distribution at X2_coil (S4 and S5 is turned off, and S6 is turned ON).

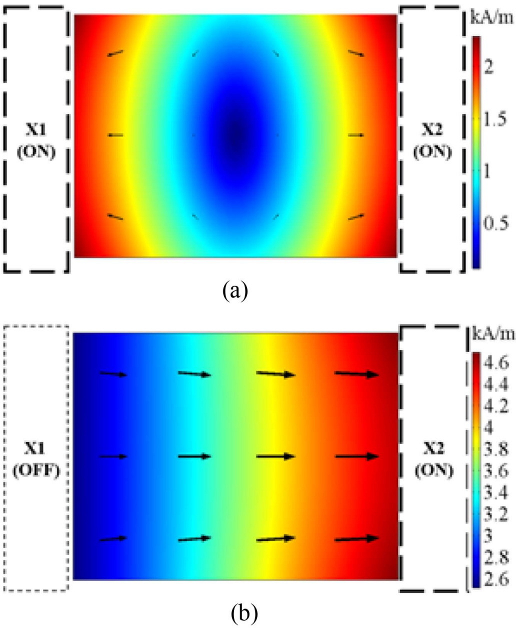

Fig. 3. (Color online) Magnetic field Difference between Maxwell coil and a single coil: (a) Gradient magnetic field of Maxwell coil and (b) gradient magnetic field of a single coil.

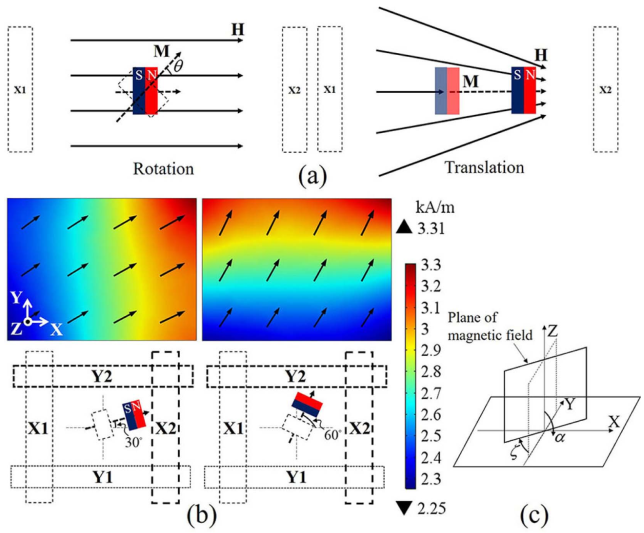

Fig. 4. (Color online) (a) Principle of magnetic torque and force control (b) method of steering function using gradient magnetic field, and (c) manipulation of plane of magnetic field using a longitude angle α and a latitude angle ζ.

the −30 mm point and 3.91 kA/m at the 30 mm point: field gradient is 0.041 mT/mm. The linearity of the gradient field is necessary factor for precise control of magnetic micro/nano robots. In general, Maxwell coil can control the range of linear gradient field, whereas a single coil can not control the range of linear gradient field. Thus, the gradient field of a single coil is suitable for a narrow working space using. Figure 3 shows simulation results of the Maxwell coil and the single coil. The linear gradient field of Maxwell coil is controlled by the position of field free region.

2.2. Magnetic field manipulation

The developed coil system can generate a uniform rotating magnetic field for magnetic torque control and a gradient magnetic field for magnetic force control by the switch conditions. Magnetic torque and force can be expressed as follows:

$$\begin{aligned} \boldsymbol{T} &= \boldsymbol{M} \times \boldsymbol{B}_{ext} \\ \boldsymbol{F} &= \nabla(\boldsymbol{M} \cdot \boldsymbol{B}_{ext}) \end{aligned} \tag{1}$$

where $\boldsymbol{M}$ is the magnetic moment, $\boldsymbol{B_{ext}}$ is the applied external magnetic field density, and $\boldsymbol{T}$ and $\boldsymbol{F}$ denote magnetic torque and force, respectively. Figure 4(a) shows the two magnetic actuations (rotation and translation) in the uniform and the gradient fields. Figure 4(b) shows gradient field distribution and the method of steering with translation motion (active locomotion) using the gradient magnetic field in the XY-plane. To obtain these conditions, the S1 and S4 is turned OFF, and the switches (S3 and S6) are turned ON. Under the conditions, X2 and Y2 coils are selected. When the steering angle ζ is 60 degrees, the applied currents of X2 and Y2 coils are 4.5 A and 2.6 A, respectively. Equation (2) and (3) represent a rotating magnetic field density $\boldsymbol{B_R}$ for magnetic torque control and a gradient magnetic field density $\boldsymbol{B_G}$ for magnetic force control, respectively.

$$\boldsymbol{B}_{\boldsymbol{R}} = \begin{pmatrix} \dfrac{\mu_0 n_x I_{mx} R_x^{\,2}}{(R_x^{\,2}+c_x^{\,2})^{3/2}}(\cos\zeta\cos\omega t+\sin\zeta\sin\alpha\sin\omega t), \\ \dfrac{\mu_0 n_y I_{my} R_y^{\,2}}{(R_y^{\,2}+c_y^{\,2})^{3/2}}(\cos\zeta\sin\alpha\sin\omega t-\sin\zeta\cos\omega t), \\ \dfrac{\mu_0 n_z I_{mz} R_z^{\,2}}{(R_z^{\,2}+c_z^{\,2})^{3/2}}(\cos\alpha\sin\omega t) \end{pmatrix} \tag{2}$$

$$\boldsymbol{B_G} = \begin{pmatrix} \dfrac{\mu_0 n_x I_y R_x^{\,2}}{2(R_x^{\,2}+c_x^{\,2})^{3/2}}\cos\alpha\cos\zeta, \\ -\dfrac{\mu_0 n_y I_y R_y^{\,2}}{2(R_y^{\,2}+c_y^{\,2})^{3/2}}\cos\alpha\sin\zeta, \\ \dfrac{\mu_0 n_z I_z R_z^{\,2}}{2(R_z^{\,2}+c_z^{\,2})^{3/2}}\sin\alpha \end{pmatrix} \tag{3}$$

where n_Δ denotes the number of turns. α and ζ denote the longitude angle and the latitude angle, respectively. R_Δ and c_Δ is the radius of Δ-axis coil and the center position of Δ coil, respectively. I_m and I_Δ is the magnitude of AC current and DC current, respectively. The angles of α and ζ change the ratio of the applied current signals, and they determine the steering direction because the different current ration changes the plane of magnetic field, as shown in Fig. 4(c).

3. Experimental Analysis

To verify performance of the proposed method, we conducted various experimental tests. In the experiments, we conducted the tests of active locomotion by magnetic force control using a cylindrical permanent magnet and hybrid control using spiral-type magnetic machine in the working space of 60 mm × 60 mm × 60 mm (uniform field area), as shown in Fig. 5. The magnetized directions of cylindrical permanent magnet and the spiral-type machine are height and radial directions, respectively. The cylindrical magnet is used in gradient magnetic field as a translational motion, whereas magnetic spiral-type machine was used for both gradient and uniform field to generate a rotational and translational motions.

Figure 5(b) shows variations of the gradient magnetic field strength when a current of 8.7 A was applied to the Y1_coil for magnetic force control. The field strengths of points 1 to 5 are 3.64, 4.06, 4.49, 4.9, and 5.3 kA/m, respectively. When moving from point 1 to point 5, the magnetic field is increased to an average of 0.41 kA/m.

The test-bed has different channel widths: W_1, W_2, and W_3 is 10, 12.45, and 7.4 mm, respectively. The machine can not move a channel narrower than the length of the machine by translational motion in the transverse direction of the machine. Therefore, the machine moves to the rotating motion in 10 mm and 7.4 mm channels, while in the 12.45 mm channel, the machine is controlled by the gradient field (translational motion). First, the spiral-type machine is driven by a rotating magnetic field (magnetic torque control), as shown in Fig. 5(c) to (f); the plane of a rotating magnetic field was changed in XZ-plane to YZ-plane to XZ plane. In this case, the S1, S4 and the S7 is turned ON for configuration of Helmholtz coil. During the magnetic torque control, the coils generated a clockwise rotating magnetic field of 5.7 kA/m with the driving frequency of 3 Hz, and the steering angle ζ was changed at intervals of 90 degrees to reach point_1. When the machine is reached at the point_1, the machine, which generates translational motion, is moved to the point_3 and the point_5 by gradient field from the Y1_coil (only S2 is turned ON), as shown in Fig. 5(g) and (i). To reach target A and B, the S1 and the S7 are turned on and the other switches are turned off to generate a rotating magnetic field in the YZ_plane. The clockwise rotation occurs forward movement and the counterclockwise rotation occurs backward movement, as shown in Fig. 5 (h) and (j). In this experiment, the proposed hybrid method efficiently controlled the machine by changing the locomotive method (torque and force control) according to the size of the channel.

The magnetic force and torque control differ not only in motion but also in speed control. The movement speed of the rotational motion is determined by the rotational frequency and the blade mechanisms, while in translational motion it is determined by gradient magnetic field strength. Figure 6(a) shows the moving velocity of the rotating motion of the spiral-type machine at the rotating field strength of 5.7 kA/m (XZ_plane) with 3 Hz, 6 Hz, and 9Hz, respectively, in a silicone oil of 500 cst. Under these conditions, the machine occurred the moving velocities of 2.2, 3.6, 4.9 mm/s, respectively. Magnetic field strength

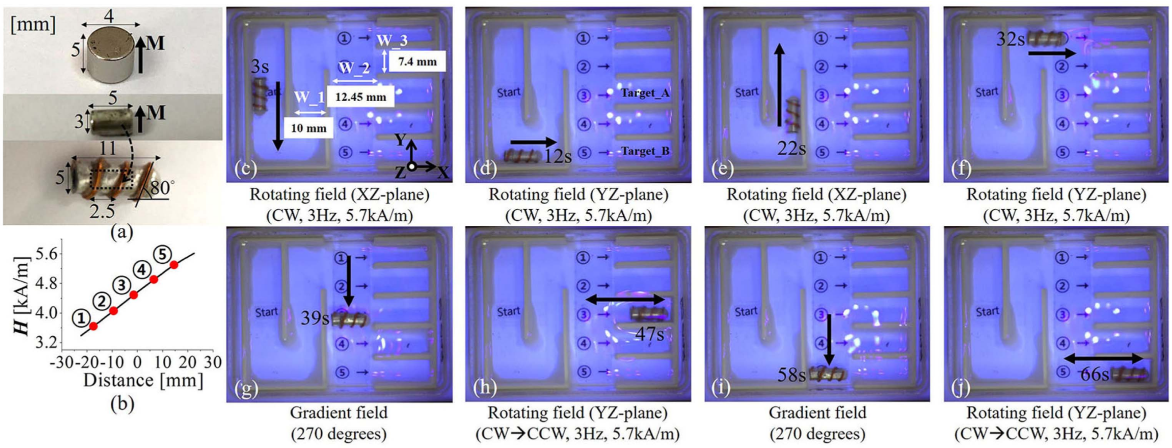

Fig. 5. (Color online) (a) Testing machines: cylindrical magnet and spiral-type machine, (b) gradient field strength from pint 1 to 5, and (c) to (j) active locomotion by a rotating magnetic field and a gradient magnetic field using switch control of the three-axis Helmholtz coil.

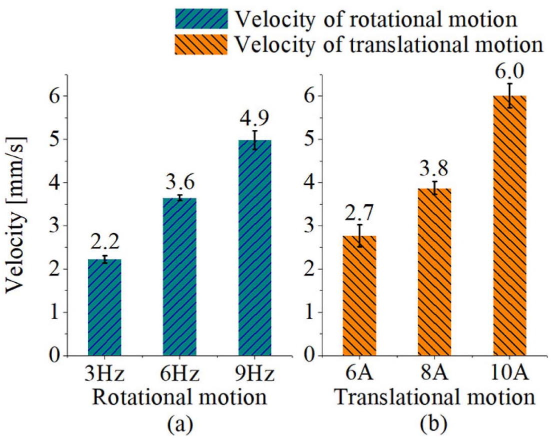

Fig. 6. (Color online) Observation of movement velocity: (a) velocity of rotating motion by magnetic torque control and (b) velocity of translational motion by gradient field.

can change the step-put point and does not affect the moving speed. Figure 6(b) shows the moving velocity by the changes in gradient field. The applied currents of 6 A, 8 A, and 10 A generated the maximum speeds of 2.7, 3.8, and 6.0 mm/s, respectively. If the field strength is large, it has a large rate of change of the moving speed. The maximum speed difference between the driving currents of 6 A and 8 A was 1.1 mm/s and the speed difference was 2.2 mm/s at the currents of 8 A and 10 A. The moving speed of the machine by rotation increased in proportion to the driving frequency; the increase of 3 Hz interval showed an average increase of 1.35 mm/s.

To verify steering function using gradient field control, we utilized a cylindrical permanent magnet. When we change the steering angle ζ, the driving currents and the coils are automatically determined by Eq. (3). Figure 7(a) shows that the magnet moves to reach the point P3 through the translational motion: the gradient field direction is 315 degrees. To generate the field direction of 315 degrees, the S2 and the S6 are turned on and the other switches are turned off. Under these conditions, the Y1_coil and the X2_coil are selected and the driving currents are 6.38 A and 7.54 A, respectively. Under the condition, magnetic field strength between P1 and P3 points are 4.6 kA/m and 5.7 kA/m: the gradient is 0.025 mT/mm. In order to move the magnet to the P2, the direction of the magnetic field is changed to 90 degrees. At this time, S3 is turned on and the other is turned off. When 9.8 A is applied to Y2_coil, the field strengths of P2 and P3 are 4.1 and 6.1 kA/m: the gradient is 0.075 mT/mm. Under the experiment, we observed control error of steering and trajectory according to changes in control angle. When the applied gradient fields were 45° and 225°, the maximum error was 8 % and the minimum error was 3 %.

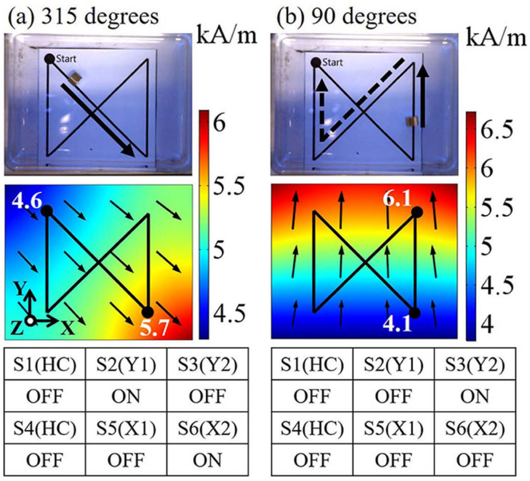

Fig. 7. (Color online) Observation of steering function by gradient magnetic field: (a) conditions for field direction of 315 degrees (b) conditions for field direction from 315 to 90 degrees.

4. Discussion and Conclusion

In this study, we have tested and verified a hybrid control system that performs magnetic force control and magnetic torque control by switching three-axis Helmholtz coils. The hybrid control method generates a uniform rotating field or a gradient field according to switch conditions. The system configuration of the proposed method is simplified in comparison with the conventional method because there is no need for a Maxwell coil to generate a gradient field. The advantage of hybrid control is that it is very useful when the size of the channel varies. Therefore, we fabricated a channel that is larger and smaller than the size of the machine and experimentally verified it using a spiral-type machine. Magnetic torque control generates a rotating magnetic field in the Helmholtz coils to move the machine in the direction of the rotational axis. Thus, it is suitable when the width of the channel is less than the length of the machine. For magnetic force control, the Helmholtz coils are separated to create a gradient field. In addition, it can move the machine quickly through translational motion when the width of the channel is wider than the length of the machine. We were able to select rotational or translational motions in 3-axis Helmholtz coil through switch control.

Acknowledgments

This research was supported by Wonkwang University in 2018.

References

[1] J. J. Abbott, K. E. Peyer, M. C. Lagomarsino, L. Zhang, L. X. Dong, I. K. Kaliakatsos, and B. J. Nelson, Int. J. Robot. Res. **28**, 1434 (2009).
[2] S. H. Kim, S. Hashi, and K. Ishiyama, J. Appl. Physi.. **109**, 07E318 (2011).
[3] A. Ghosh and P. Fischer, Nano Lett. **9**, 2243 (2009).
[4] S. H. Kim and K. Ishiyama, IEEE Trans. Mechatronics. **19**, 1651 (2013).
[5] B. J. Nelson, I. K. Kaliakatsos, and J. J. Abbott, Annual Review of Biomedical Engineering. **12**. 55 (2010).
[6] S. Yim and M. Sitti, IEEE. Trans. Robotics **28**, 183 (2011).
[7] C. H. Yu and S. H. Kim, J. Magn. **22**, 162 (2017).
[8] K. Ishiyama, M. Sendoh, A. Yamazaki, and K. I. Arai, Sens. Actuators A **91**, 141 (2001).
[9] S. M. Jeong and G. H. Jang, IEEE Trans. Magn. **48**, 4062 (2012).
[10] S. Sudo, S. Segawa, and T. Honda, J. Intell. Mater. Syst. Structure **17**, 729 (2006).
[11] K. Ishiyama, M. Sendoh, and K. I. Arai, JMMM. **242-245**, 41 (2002).
[12] M. T. Hou, H. M. Shen, G. L. Jiang, C. N. Lu, I. J. Hsu, and J. A. Yeh, Appl. Phys. Lett. **96**, 024102 (2010).
[13] T. Honda, K. I. Arai, and K. Ishiyama, IEEE Trans. Magn. **32**, 5085 (1996).
[14] J. J. Abbott, O. Ergeneman, M. P. Kummer, A. M. Hirt, and B. J. Nelson, IEEE Trans. Robot. **23**, 1247 (2007).
[15] S. H. Kim, S. Hashi, and K. Ishiyama, Smart Mater. Struct. **22**, 027001 (2013).
[16] S. H. Kim, K. Shin, S. Hashi, and K. Ishiyama, Bioinspir. Biomim. **7**, 036007 (2012).